Temporal lung changes in high-resolution chest computed tomography for coronavirus disease 2019

Chengyang Chen (iD)**, Xing Wang, Jia Dong, Dianer Nie, Qianlan Chen, Feng Yang, Weiwei Chen* and Qiongjie Hu*** (iD)

Abstract

Objective: To evaluate temporal lung changes in coronavirus disease 2019 (COVID-19) in high-resolution computed tomography (HRCT) and to determine the appropriate computed tomographic (CT) follow-up time.

Methods: Eighty-six patients with two or more HRCT scans who were diagnosed with COVID-19 were included. The CT score and major CT findings were evaluated.

Results: Eighty-two (95.3%) patients had lesions on the initial HRCT scans. Most scans showed bilateral, multifocal lung lesions, with multiple lobes involved and diffuse distribution. For fifty-seven patients with type I (progress compared with the initial CT score), the CT score reached a peak at 12 days and the nadir at 36 days. For twenty-nine patients with type II (no progress compared with the initial CT score), the lowest CT score was reached at 23 days. On the final HRCT scans (>21 days), patients with a reticular pattern were older than those without a reticular pattern.

Conclusion: The appropriate follow-up time of CT scans is during the second week (approximately 12 days) and the fourth to fifth weeks (approximately 23–36 days) from the onset of illness. These times could help reduce the CT radiation dose and show timely changes in the course of the disease by CT.

Department of Radiology, Tongji Hospital, Tongji Medical College, Huazhong University of Science and Technology, Wuhan, China

*These authors contributed equally to this work.

Corresponding author:
Qiongjie Hu, Department of Radiology, Tongji Hospital, Tongji Medical College, Huazhong University of Science and Technology, 1095 Jiefang Avenue, Hankou District, Wuhan 430030, China.
Email: qjhu@outlook.com

Introduction

Beginning in December 2019 in Wuhan City, Hubei Province, China reported a series of unexplained cases of pneumonia, which were initially related to exposure of the Wuhan South China Seafood Wholesale Market.[1] This pneumonia was then found to be a new acute viral respiratory disease (coronavirus disease 2019 [COVID-19]), which was caused by a new coronavirus (severe acute respiratory syndrome coronavirus-2 [SARS-CoV-2]).[2] Similar to other coronaviral pneumonias, such as severe acute respiratory syndrome caused by coronavirus and Middle East respiratory syndrome coronavirus, COVID-19 can also lead to acute respiratory distress syndrome.[1,3,4] On the basis of the current epidemic, COVID-19 was more infectious than SARS-CoV.[2] By 19:42 on 17 March 2020, 81,135 confirmed cases of COVID-19 and 3231 deaths had been reported in China. Except for China, 104,089 confirmed cases of COVID-19 and 4184 deaths had been reported in 157 countries and regions. With the gradual recognition of COVID-19 pneumonia, professional consensus, guidelines, and criteria have steadily been established for the purpose of preventing transmission and facilitating diagnosis and treatment.[4] In this process, computed tomography (CT) had become the main screening and reviewing method for COVID-19 pneumonia because of its high specificity and sensitivity.[5] However, owing to the radiation effect of CT, the increased number of screening and reexamination times, and the greater radiation dose to the human body, this might cause different degrees of sequelae, such as cancer.[6]

The present study aimed to examine the changes in chest CT manifestations of this pneumonia from the onset of initial symptoms to various time points in outpatients with COVID-19 pneumonia in Wuhan, China. We also aimed to examine the relationship between the time from the onset of initial symptoms and changes in the CT score, and then to determine the appropriate CT follow-up time.

Patients and methods

Patients

This study was approved by the Institutional Review Board (IRB) of Tongji Hospital, Tongji Medical College, Huazhong University of Science and Technology (IRB ID: TJ-C0200108). The study was performed in accordance with the 1964 Helsinki Declaration and its later amendments or comparable ethical standards. Written informed consent was obtained from all patients in this retrospective study. Anonymous data were collected and analyzed to facilitate better clinical decisions and treatment.

Patients with COVID-19 pneumonia in the outpatient clinic were enrolled retrospectively from 14 January to 16 March 2020 in this single-center study. A flow chart of the selection criteria is shown in Figure 1.

High-resolution CT scans

All high-resolution computed tomographic (HRCT) scans of the thorax were performed with CT scanners (GE Healthcare, Philips, or Toshiba Medical Systems, Wuhan City, Hubei Province, China) under the appropriate control conditions. These conditions were as follows: 80 to 120 kVp, automated tube current modulation of 60 to 300 mA, rotation time of 0.5 s, pitch of 0.984:1, and a slice thickness of 1.25 mm, with selected differences according to machine types. Patients were in the supine position during end-inspiration.

Interpretation of images

Two experienced radiologists reviewed the HRCT images on a picture archiving and communication system workstation
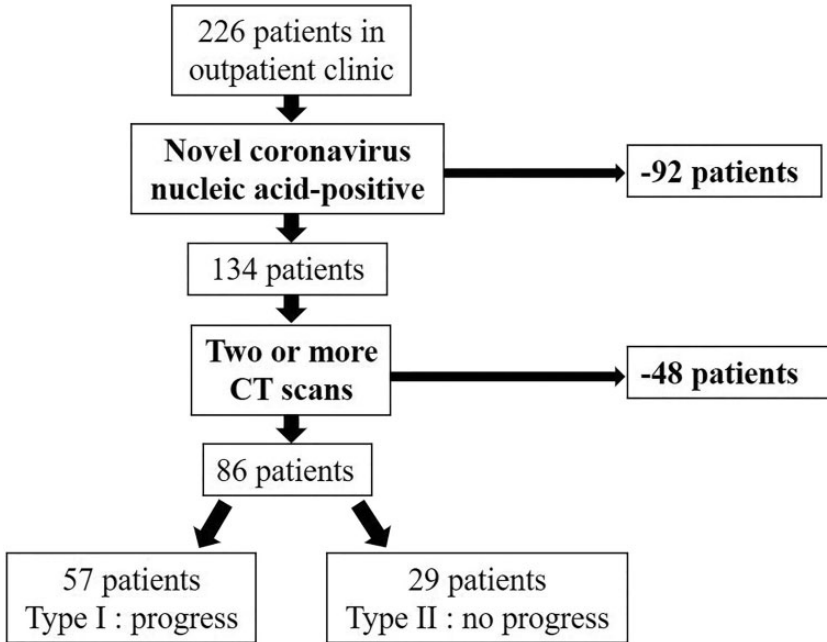
Figure 1. Flow chart of the selection criteria of patients with coronavirus disease 2019 pneumonia.

(Synapses; Fujifilm, Wuhan City, Hubei Province, China) with multiplanar reconstruction tools and reached a decision in consensus. These two radiologists had 4 and 10 years of experience in thoracic radiology. The images were viewed in lung window settings (width, 1000–1500 HU; level, 700 to −550 HU) and mediastinal window settings (width, 300–350 HU; level, 30–40 HU). Using the terms defined by the Fleischner Society and peer-reviewed literature on viral pneumonia,[4,7] the observers categorized the predominant patterns of abnormality on CT scans as pure ground-glass opacity (GGO) (hazy areas of increased attenuation without obscuration of the underlying vessels, pure GGO), predominant GGO, GGO with superimposed linear opacities (crazy-paving pattern), pure consolidation (homogeneous opacity of the parenchyma with obscuration of the underlying vessels), predominant consolidation, microvascular dilation, a stripe pattern, and a reticular pattern. On the scans, the presence of mediastinal lymphadenopathy (defined as a lymph node ≥ 1 cm in the short-axis diameter), pneumothorax, pleural effusion, and pericardial effusion was also noted. The distribution of opacity was also defined as being pure subpleural (involving only the peripheral one third of the lungs), pure central (involving only the central two thirds of the lungs), and diffuse (without predilection for being subpleural in the center regions).

The extent of disease on HRCT was also evaluated. Each lung was divided into the following three lung zones: upper (above the carina), middle (below the carina up to the inferior pulmonary vein), and lower (below the inferior pulmonary vein) zones. Each lung zone (total of six lung zones) was assigned a score that was based on the following: score of 0, 0% involvement; score of 1, <25% involvement; score of 2, 25% to <50% involvement; score of 3, 50% to

<75% involvement; and score of 4, ≥75% involvement. Summation of the scores provided overall lung involvement (maximal CT score for both lungs was 24).[8]

At review of the follow-up CT score, we were able to identify two patterns of CT scores on the basis of changes from the initial scan to the first reexamination as follows: type I, progress compared with the initial CT score; and type II, no progress compared with the initial CT score. We also examined the relationship between the follow-up time and the change in CT score of patients. Additionally, we counted the proportion of patients who showed progress each week to determine the appropriate CT follow-up time. For all patients, we also recorded imaging characteristics of the last HRCT scan and determined if there was any lesion that was completely absorbed during the follow-up period.

Statistical analysis

The median values of the CT score and temporal changes in the main CT patterns were analyzed. Quantitative data are presented as mean ± standard deviation and median (minimum–maximum). Count data are presented as the percentage of the total unless otherwise specified. The change in CT score of the lungs as a function of time was quantitatively assessed using the R curve estimation module. Data were evaluated by the t test, Mann–Whitney U test, χ^2 test, or Fisher's exact test, as appropriate. A P value of <0.05 was defined as statistically significant. Statistical analyses were performed using R software (version 3.6.1, the R Foundation for Statistical Computing, Vienna, Austria).

Results

Baseline characteristics of the patients

The patients included 32 men and 54 women, aged 15 to 78 years, with a mean (± standard deviation) age of 50 ± 15 years. Of these patients, 25 (29.1%) were aged >60 years, with a mean age of 68 ± 5 years. The most common clinical manifestation was fever, followed by cough, fatigue, muscle pain, headache, and chest pain (Table 1).

Imaging characteristics of initial HRCT

Of the eighty-six patients with COVID-19 included in this study, 82 (95.3%) showed abnormalities in the first pulmonary HRCT scan (Table 2). Most patients showed multiple lobes involved, and in patients aged >60 years, most (25/25, 100%) of them showed multiple lobes involved. More than half of the patients presented with bilateral, multifocal lung lesions, with diffuse distribution. Among patients aged >60 years, 17 (17/25, 68.0%) showed this distribution.

Various patterns of GGO were found in the patients, with coexistence of two or

Table 1. Characteristics of the patient cohort.

	All patients (n = 86)
Age (years)	50 ± 15 (15–78)
Sex	
Male	32 (37.2)
Female	54 (62.8)
Initial symptoms	
Fever (temperature >37.3°C)	64 (74.4)
Cough	39 (45.3)
Fatigue	18 (20.9)
Muscle pain	10 (11.6)
Headache	3 (3.5)
Chest pain	1 (1.2)
Number of CT scans	3 ± 1 (2–8)
Period between the onset of initial symptoms and the first CT scan (days)	5 ± 2 (2–9)
Interval between the onset of initial symptoms and the last CT scan (days)	27 ± 23 (7–96)

Quantitative data are presented as mean ± standard deviation (minimum–maximum) and count data are presented as number (%). CT, computed tomography.

Table 2. Imaging characteristics of initial high-resolution computed tomography.

Patients (n = 86)	
Distribution	
Peripheral distribution	17 (19.7)
Central distribution	5 (5.8)
Diffuse distribution	60 (69.8)
Unilateral involvement	14 (16.3)
Right lung	13 (15.1)
Left lung	1 (1.2)
Bilateral involvement	68 (79.0)
Number of lung lesions	
Unifocal lesion	7 (8.1)
Multifocal lesions	75 (87.2)
Number of lobes involved	
0	4 (4.7)
1	8 (9.3)
2 or more	74 (86.0)
Patterns of the lesion	
Pure GGO	4 (4.7)
Predominant GGO	13 (15.1)
Crazy-paving pattern	33 (38.4)
Predominant consolidation	32 (37.2)
Coexistence of two or more forms	29 (33.7)
Other signs in the lesion	
Stripe pattern	17 (19.8)
Microvascular dilation	81 (94.2)
Other findings	
Mediastinal lymphadenopathy	15 (17.4)
Pericardial effusion	1 (1.2)

Count data are presented as number (%). GGO, ground glass opacity

more forms in 29 (33.7%) patients. Microvascular dilation, mediastinal lymphadenopathy, and pericardial effusion were observed. Of the patients aged >60 years, 11 (11/25, 44.0%) showed the coexistence of two or more forms of GGO and 10 (10/25, 40.0%) presented with mediastinal lymphadenopathy.
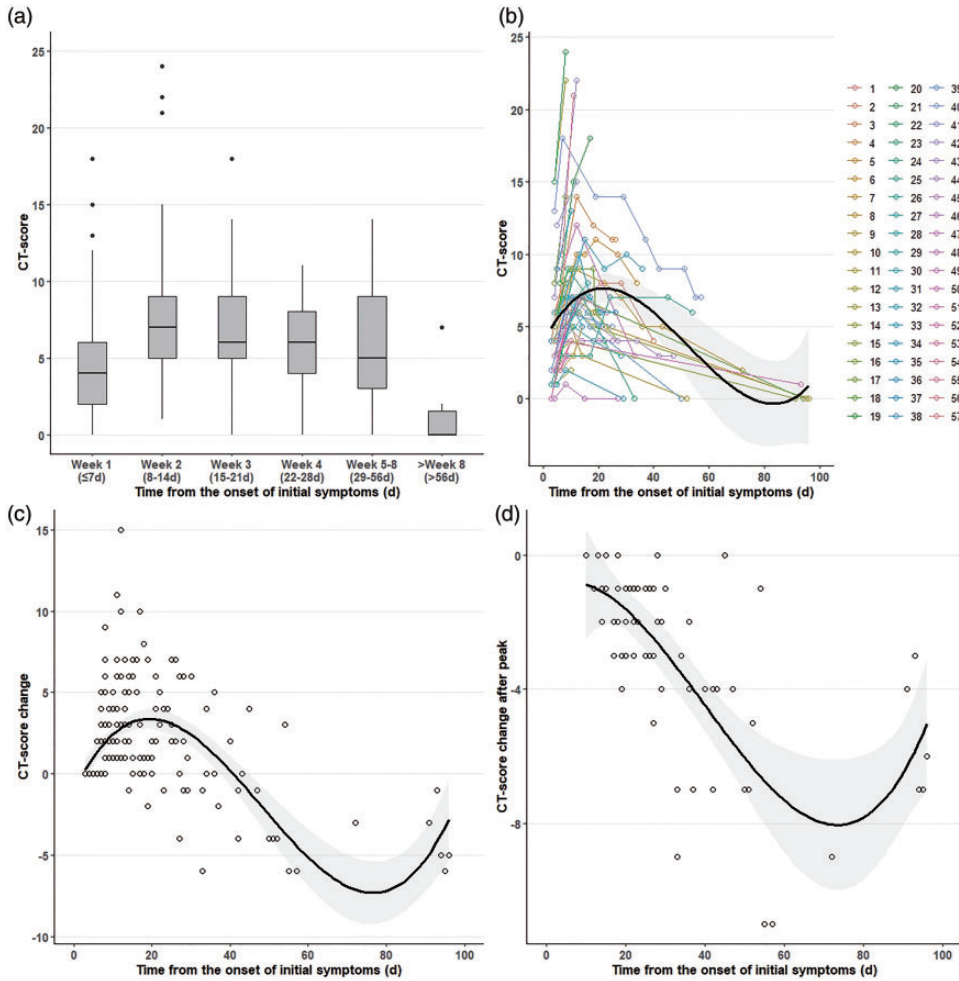
Temporal changes in CT scores

Fifty-seven patients (57/86, 66.3%, mean age: 50 ± 15 years, range: 15–75 years) showed type I and 29 (29/86, 33.7%, mean age: 49 ± 15 years, range: 26–78 years) showed type II patterns of the CT score.

Type I: progress compared with the initial CT score. A total of 199 CT scans were performed, of which the mean time from onset of illness to the initial scan was 4 ± 1 days. There was a marked increase in the median CT score after onset of symptoms (Figure 2a). The median CT score peaked during the second week (8–14 days) of illness, with a median value of 7 (range: 1–24). After this time, the median CT score slightly dropped to 6 (range: 0–18) during the third week (15–21 days) of illness, and remained at this level until the fifth to eighth weeks (29–55 days) of illness before falling further slowly. The median CT score dropped to close to 0 after 8 weeks (>56 days) of illness. Changes in the CT score for every patient with type I are shown in Figure 2b. With regard to the change in CT score (follow-up CT score – the initial CT score), the mean peak value (Figure 2c) was reached at 12 ± 3 days of illness. Among the fifty-seven patients with type I, temporal changes in the CT score after reaching a peak (follow-up CT score – peak CT score) are shown in Figure 2d. The mean nadir was reached at 36 ± 25 days of illness.

Eight (8/57, 14.0%) patients showed progress during the first week (≤ 7 days) of illness, 50 (50/57, 87.7%) showed progress during the second week of illness, and three patients showed progress during the third week of illness compared with the initial CT score. Among them, four patients had more severe progression and CT showed "white lung" sign (Figure 3). No patient showed progress during the fourth and fifth to eighth weeks, and after 8 weeks of illness.

Type II: no progress compared with the initial CT score. Ninety-four CT scans were performed, of which the mean time from onset of illness to the initial scan was 6 ± 2 days.

Figure 2. Temporal changes in the CT score in patients with a type I pattern. (a) Median change in the CT score. (b) Change in the CT score for every patient. (c) Changes in the CT score before the CT score reached a peak (d) and after this peak. Curve fitting equation: (c), $y = 0.0001 \times x3 - 0.016 \times x2 + 0.508 \times x1 - 1.141$, in which x=time from onset of the initial symptoms, y=change in the CT score (reexamination CT score − initial CT score), $R^2 = 0.32$, P<0.001; (d), $y = 0.00005 \times x3 - 0.006 \times x2 + 0.061 \times x - 0.969$, in which x=time from onset of the initial symptoms, y=change in the CT score (reexamination CT score-− peak CT score), $R^2 = 0.49$, P<0.001. CT, computed tomography; d, days.

The median CT score remained stable during the first and second weeks of illness, with a median value of 6 (range: 0–20) (Figure 4a). After this time, the median values slightly dropped. The change in CT score for every patient with the type II CT score pattern is shown in Figure 4b. With regard to the change in CT score (Figure 4c), the mean nadir was reached at 23 ± 13 days.
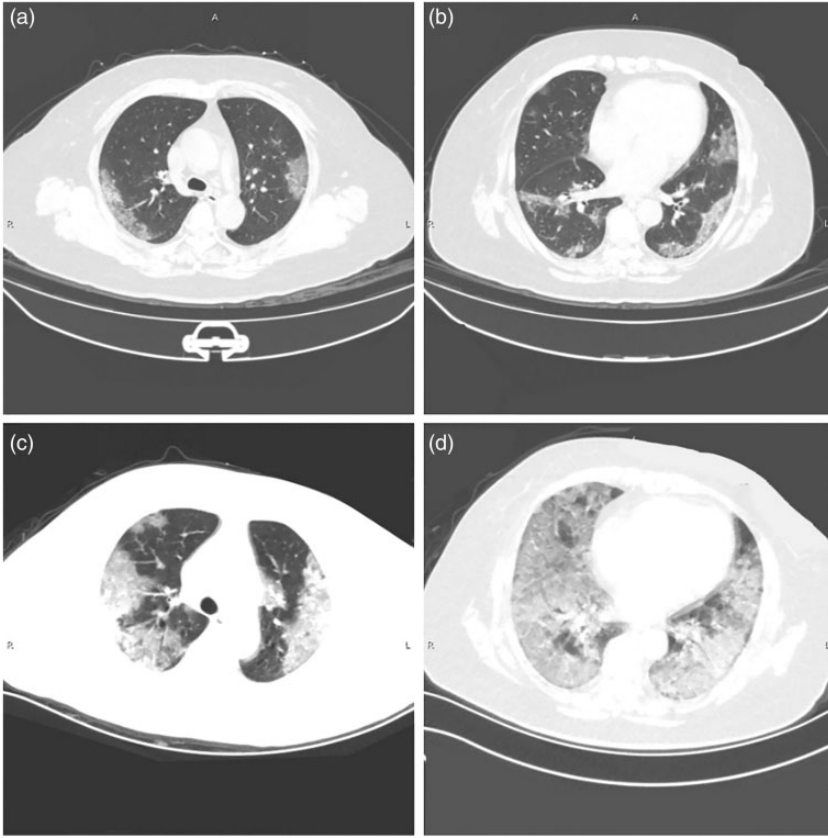
Figure 3. (a, b) High-resolution computed tomography of a 57-year-old woman at the first computed tomographic scan. There is scattered predominant round-glass opacity in the peripheral zone of both lungs. (c, d) High-resolution computed tomography at the first reexamination after 8 days. Diffuse crazy-paving pattern with partial consolidation in both lungs can be seen, showing white lung changes.

Temporal changes in main CT patterns

The temporal changes in main CT patterns for patients with type I (fifty-seven patients with 199 CT scans) and type II (twenty-nine patients with 94 CT scans) are shown in Figure 5. The predominant pattern of abnormality for both types was the crazy-paving pattern during the first week of illness and predominant consolidation during the second week of illness. After this time, the crazy-paving pattern and predominant consolidation were partially or totally absorbed and the percentage of GGO and a normal pattern increased.

Imaging characteristics of the final HRCT scan during follow-up

The mean interval between the onset of initial symptoms and the final CT scan was 27 ± 23 days (range: 7–96 days). During this period, there was a 28-year-old female patient (1.2%) without any lesion during the 50 days of follow-up (Figure 6). The lesion was completely absorbed in 12 (12/86, 14.0%) patients who had a mean age of 43 ± 15 years and the mean time from onset of illness was 65 ± 32 days. The lesion was partially absorbed in 73 (73/86, 84.8%) patients in whom the mean
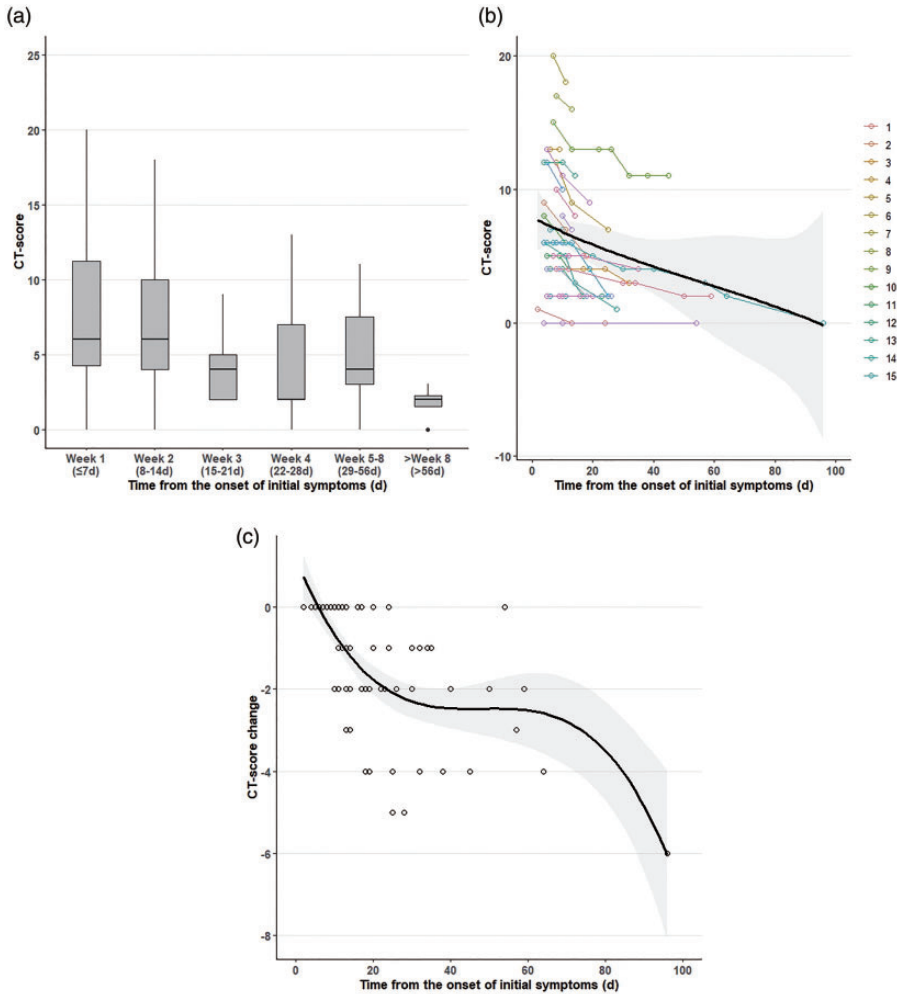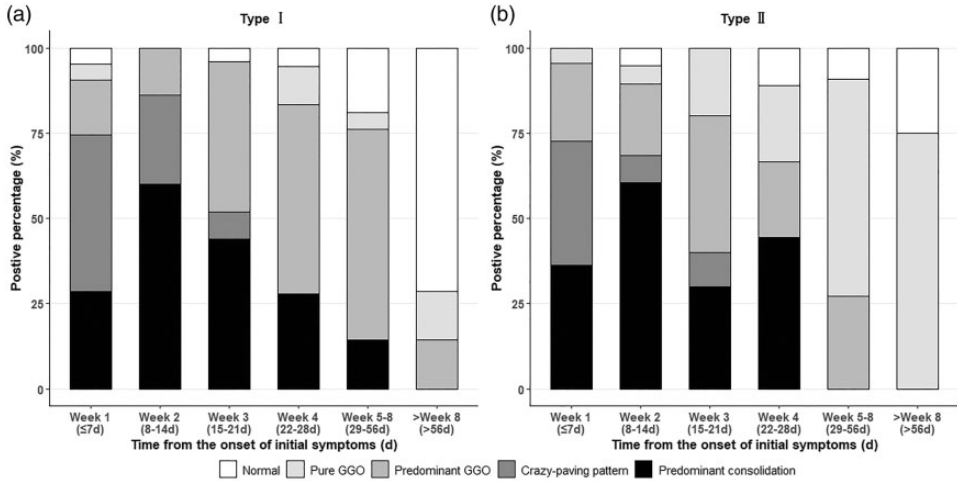
Figure 4. Temporal changes in the CT score in patients with a type II pattern. (a) Median change in the CT score. (b) Changes in the CT score for every patient. (c) Scatterplot showing changes between the reexamination CT score and the initial CT score. (c). Curve fitting equation:
$y = -0.00003 \times x3 + 0.005 \times x2 - 0.229 \times x1 + 1.164$, in which x=time from onset of the initial symptoms, y=change in the CT score (reexamination CT score − initial CT score), R^2=0.51, P<0.001. CT, computed tomography; d, days.

age was 51 ± 14 years (P=0.042 vs patients with completely absorbed lesions) and the mean time from onset of illness was 20 ± 14 days (P<0.001 vs patients with completely absorbed lesions). On the last HRCT scans (>21 days), pure GGO was found in 7 (7/37, 18.9%) patients, predominant GGO in 13 (13/37, 35.1%), predominant consolidation in 4 (4/37, 10.8%), and a normal pattern in 13 (13/37, 35.1%). Fifteen (15/37, 40.5%) patients showed a reticular pattern (Figure 7) in whom the mean age was 63 ± 10 years, which was older than that of those without a reticular pattern (mean age: 42 ± 13 years, P<0.001).

Figure 5. Temporal changes in the main computed tomographic patterns. Stacked bar graphs show the distribution of the main patterns of lung abnormalities in patients with types I (a) and II (b) computed tomographic score patterns at various time points from the onset of symptoms. GGO, ground-glass opacity, d, days.

Discussion

COVID-19 disease is a new, highly infectious, viral pneumonia that is caused by a novel coronavirus (SARS-CoV-2) of unknown origin. In this study, we observed eighty-six outpatients who were diagnosed with COVID-19 pneumonia. Among them, the predominant clinical manifestations were fever (74.4%), cough (45.3%), and fatigue (20.9%). More than half of the patients showed bilateral, multifocal lung lesions, with multiple lobes involved and diffuse distribution. Fourteen patients presented with unilateral lesions, of these patients, thirteen patients had unilateral lesions which occurred in the right lung. This finding might be because of the innate anatomical features of the right lung bronchus.[2] On CT images, COVID-19 pneumonia had a mixed pattern involving lung parenchyma and lung interstitium.[9] The virus first invaded the pulmonary interstitium, which was characterized by edema and thickening of the interlobular septum, interlobular interstitium, subpleural interstitium, interlobular central interstitium,

and peribronchovascular interstitium. This manifested as GGO and a crazy-paving pattern. Consolidation might represent further infiltration of the parenchyma. Microvascular dilation sign might indicate increased blood supply to the inflammatory area of the lungs.[2] Patients older than 60 years often presented with multifocal lung lesions, multiple patterns of abnormality, diffuse distribution involving multiple lobes, and mediastinal lymphadenopathy. This finding might be related to the fact that older people have more basic diseases.

CT has become the main screening and reviewing method for COVID-19 pneumonia because of its high specificity and sensitivity. Each patient needed to have multiple CT examinations during the course of this disease in our study. Therefore, physicians should pay attention to the radiation effects of CT examinations. Although a chest X-ray delivers a radiation dosage of approximately 0.05 mSv, a standard chest CT might deliver approximately 4 to 7 mSv. One CT scan might be associated with an oncogenic risk of 0.05% to 0.7%. For
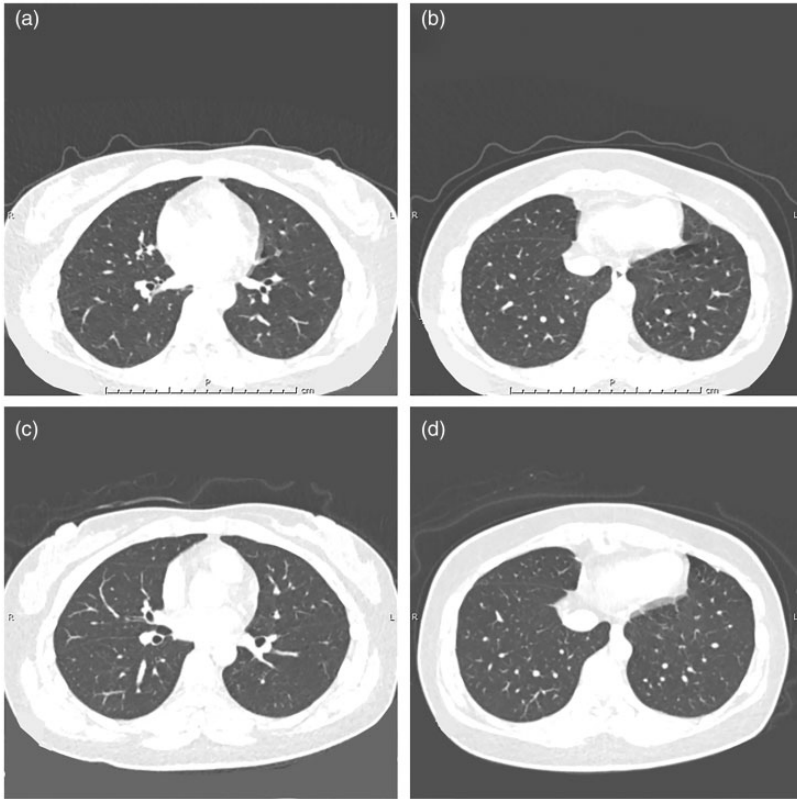
Figure 6. (a, b) High-resolution computed tomography of a 28-year-old woman at the first diagnosis. No lesion can be seen in both lungs. (c) High-resolution computed tomographic findings of the first reexamination after 50 days. There is still no lesion in the lungs.
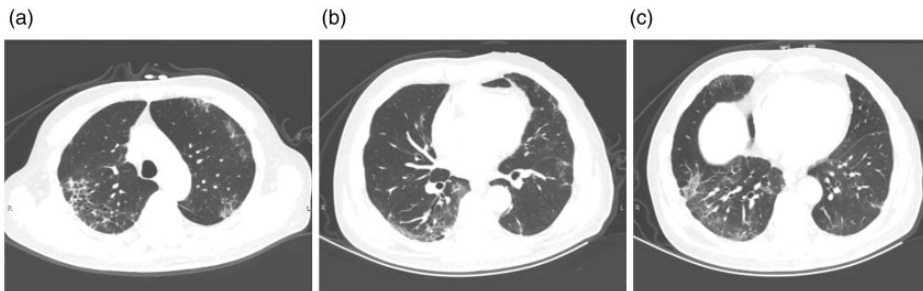
Figure 7. (a–c) High-resolution computed tomographic findings of a 73-year-old male patient during outpatient follow-up. A multiple reticular pattern can be seen around the right lower lobe stripe pattern.

patients who have multiple CT scans, the risk could be as high as >2.7%. Moreover, a CT scan incurs procedure-induced viral transmission.[6,10] Therefore, we should reduce the number of examinations or change to X-rays with a lower radiation dose while ensuring the effectiveness of CT examinations to reduce the effect of

radiation. Therefore, in the current study, we examined the changes in CT follow-up at different times to determine the appropriate follow-up interval.

After completing the first CT scan, we found that patients should undergo CT reexamination when the change in CT score (follow-up CT-score − initial CT score) reached its peak (or low) value to reduce the CT radiation dose. For fifty-seven patients with the type I CT score pattern, the CT score and the change in CT score reached a peak at a mean of 12 days from onset of illness, and the proportion of patients who showed progress reached the peak value during the second week of illness. This finding is consistent with the results of other studies.[4,11] Furthermore, the change in CT score after it reached a peak (follow-up CT score − peak CT score) was determined, with low values at approximately 36 days from the onset of illness. Therefore, for most patients with type I (conditions continued to progress), a CT reexamination at approximately 12 days from onset of illness is recommended. After this time when the disease course is in remission, a CT reexamination at approximately 36 days from the onset of illness is recommended. For twenty-nine patients with a type II CT score pattern, the nadir of a change in CT score was reached at a mean time of 23 days from the onset of illness. Therefore, a CT reexamination is recommended at this time. All recommendations were made to reduce the CT radiation dose of patients and to show timely changes in CT in the course of the disease.

In our study, we observed the imaging characteristics of the final HRCT scan during follow-up. The mean age and the follow-up of patients with completely absorbed lesions were younger and longer, respectively, than those in patients with partially absorbed lesions. This finding suggested that younger patients and a longer follow-up are associated with easier absorption of lesions. We also found that older patients were more likely to have a reticular pattern (a sign of pulmonary fibrosis) than younger patients.

The present study has three limitations. First, the sample size for this experiment was relatively insufficient. Therefore, a larger sample size is required in future studies. Second, because we enrolled outpatients, detailed clinical data and laboratory findings of patients were relatively lacking. Third, because no suitable software was found, we did not use AI software for segmentation of lesion volume. This should be our next research direction.

In conclusion, for patients with a type I pattern (progress compared with the initial CT score), the appropriate follow-up time of CT scans is during the second week (approximately 12 days) and the fifth week (approximately 36 days) from the onset of illness. In the former time, patients are in progression of the disease and a CT reexamination aims to help determine the extent of the disease, while in the latter time, patients are in recovery and a reexamination aims to determine absorption of the lesions. For patients with a type II CT score pattern who might be in recovery, the appropriate follow-up time of CT scans is during the fourth week (approximately 23 days) from the onset of illness. All recommendations aim to reduce the CT radiation dose of patients and to provide timely changes in the course of the disease using CT.

Author contributions

ORCID iDs

Chengyang Chen https://orcid.org/0000-0002-5523-8169
Qiongjie Hu https://orcid.org/0000-0001-8910-0785

References

1. Huang C, Wang Y, Li X, et al. Clinical features of patients infected with 2019 novel coronavirus in Wuhan, China. *Lancet* 2020; 395: 497–506. DOI: 10.1016/s0140-6736(20)30183-5.
2. Zhou S, Wang Y, Zhu T, et al. CT Features of Coronavirus Disease 2019 (COVID-19) Pneumonia in 62 Patients in Wuhan, China. *AJR Am J Roentgenol* 2020; 214: 1287–1294. DOI: 10.2214/AJR.20.22975.
3. Graham RL, Donaldson EF and Baric RS. A decade after SARS: strategies for controlling emerging coronaviruses. *Nat Rev Microbiol* 2013; 11: 836–848. DOI: 10.1038/nrmicro3143.
4. Pan F, Ye T, Sun P, et al. Time Course of Lung Changes On Chest CT During Recovery From 2019 Novel Coronavirus (COVID-19) Pneumonia. *Radiology* 2020: 295: 715–721. DOI: 10.1148/radiol.2020200370.
5. Bai HX, Hsieh B, Xiong Z, et al. Performance of radiologists in differentiating COVID-19 from viral pneumonia on chest CT. *Radiology* 2020; 296: E46–E54. DOI: 10.1148/radiol.2020200823.
6. Wang YXJ, Liu WH, Yang M, et al. The role of CT for Covid-19 patient's management remains poorly defined. *Ann Transl Med* 2020; 8: 145. DOI: 10.21037/atm.2020.02.71.
7. Ye Z, Zhang Y, Wang Y, et al. Chest CT manifestations of new coronavirus disease 2019 (COVID-19): a pictorial review. *Eur Radiol* 2020; 30: 4381–4389. DOI: 10.1007/s00330-020-06801-0.
8. Ooi GC, Khong PL, Muller NL, et al. Severe acute respiratory syndrome: temporal lung changes at thin-section CT in 30 patients. *Radiology* 2004; 230: 836–844. DOI: 10.1148/radiol.2303030853.
9. Koo HJ, Lim S, Choe J, et al. Radiographic and CT Features of Viral Pneumonia. *Radiographics* 2018; 38: 719–739. DOI: 10.1148/rg.2018170048.
10. Kalra MK, Maher MM, Rizzo S, et al. Radiation exposure from chest CT: issues and strategies. *J Korean Med Sci* 2004; 19: 159–166. DOI: 10.3346/jkms.2004.19.2.159.
11. Wang Y, Dong C, Hu Y, et al. Temporal Changes of CT Findings in 90 Patients with COVID-19 Pneumonia: A Longitudinal Study. *Radiology* 2020; 296: E55–E64. DOI: 10.1148/radiol.2020200843.